Two-Dimensional NMR Evidence for Cleavage of Lignin and Xylan Substituents in Wheat Straw Through Hydrothermal Pretreatment and Enzymatic Hydrolysis

**Daniel J. Yelle · Prasad Kaparaju ·
Christopher G. Hunt · Kolby Hirth · Hoon Kim.
John Ralph · Claus Felby**

Abstract Solution-state two-dimensional (2D) nuclear magnetic resonance (NMR) spectroscopy of plant cell walls is a powerful tool for characterizing changes in cell wall chemistry during the hydrothermal pretreatment process of wheat straw for second-generation bioethanol production. One-bond $^{13}C-^{1}H$ NMR correlation spectroscopy, via an heteronuclear single quantum coherence experiment, revealed substantial lignin ß-aryl ether cleavage, deacetylation via cleavage of the natural acetates at the 2-O- and 3-O-positions of xylan, and uronic acid depletion via cleavage of the $(1{\rightarrow}2)$-linked 4-O-methyl-α-D-glucuronic acid of xylan. In the polysaccharide anomeric region, decreases in the minor ß-D-mannopyranosyl, and α-L-arabinofuranosyl units were observed in the NMR spectra from hydrothermally pretreated wheat straw. The aromatic region indicated only minor changes to the aromatic structures during the process (e.g., further deacylation revealed by the depletion in ferulate and p-coumarate structures). Supplementary chemical analyses showed that the hydrothermal pretreatment increased the cellulose and lignin concentration with partial removal of extractives and hemicelluloses. The subsequent enzymatic hydrolysis incurred further deacetylation of the xylan, leaving approximately 10% of acetate intact based on the weight of original wheat straw.

Keywords Wheat straw · Hydrothermal · Lignin · Polysaccharides · O-acetyls · ß-aryl ethers · Uronic acids Cinnamates

Abbreviations

2D NMR	two-dimensional (solution state) nuclear magnetic resonance spectroscopy
HSQC	heteronuclear single quantum coherence
ß-D-Xyl$p$	ß-D-xylopyranosyl units
2-O-Ac-ß-D-Xyl$p$, 3-O-Ac-ß-D-Xyl$p$	O-acetylated ß-D-xylopyranosyl units
4-O-MeGlcA	4-O-methyl-α-D-glucuronic acid units
ß-D-Man$p$	ß-D-mannopyranosyl units
α-L-Ara$f$	α-L-arabinofuranosyl units
SEM	scanning electron microscope

D. J. Yelle(✉) ·C. G. Hunt · K. Hirth
U.S. Forest Service, Forest Products Laboratory,
Madison, WI, USA
e-mail: dyelle@fs.fed.us

P. Kaparaju · C. Felby
Forest & Landscape, Faculty of Life Sciences,
University of Copenhagen,
Frederiksberg, Denmark

H. Kim · J. Ralph
Department of Biochemistry, DOE Great Lakes Bioenergy
Research Center, and Wisconsin Bioenergy Initiative,
University of Wisconsin,
Madison, WI, USA

P. Kaparaju
Department of Biological and Environmental Science,
University of Jyväskylä,
Jyväskylä, Finland

Introduction

With an increased focus on the use of plant materials as substitutes for fossil fuel resources, the characterization of plant cell wall polymer structures is vital to provide the fundamental knowledge required for the development of biomass-based renewable energy technologies. In this paper, we report on the chemical structure of wheat straw from one of the first large-scale second-generation bioethanol processes [1]. The wheat straw, presoaked in water, is pretreated by simply heating to 195 ℃, producing a substrate

Springer

which is amenable to subsequent enzymatic hydrolysis and fermentation. Here, we elucidate the structural changes that occur after hydrothermal pretreatment and subsequent enzymatic hydrolysis of wheat straw with a focus on the major lignin and polysaccharide components.

Traditional analyses of plant cell wall constituents require fractionation, with the isolation of each component to obtain qualitative and/or quantitative information about its composition and structure. However, component isolation procedures lead to alterations in native cell wall chemistry (via, e.g., deacylation, oxidation, or other degradative processes) [2, 3]. It is now possible to analyze lignin polymers in ball-milled plant cell walls, without the need to separate the lignin from the polysaccharides [4], with the caveat that ball milling will decrease cellulose crystallinity [5, 6] and alter the lignin polymer structure to a certain degree based upon the milling conditions [7, 8]. Through nondegadative dissolution of ball-milled wood cell wall material in dimethylsulfoxide (DMSO) and N-methylimidazole (NMI), and in situ acetylation, two-dimensional nuclear magnetic resonance (2D NMR) was used to characterize lignin structures in considerable detail. Recently, utilizing the DMSO and NMI dissolution chemistry, wood and plant cell walls were characterized by 2D NMR in the perdeuterated solvents DMSO-d_6 and NMI-d_6 [9]. This allowed characterization of the native chemistry of the cell wall, including natural acetates found on lignin syringyl units and acetyl side groups found acylating xylan and mannan units in hemicelluloses of *Pinus taeda, Populus tremuloides,* and *Hibiscus cannabinus*. In a further simplified method, DMSO-d_6 was added directly to ball-milled wood and plant cell walls in an NMR tube to obtain a gel [10]. Although cellulose will not completely dissolve in this system, 2D NMR of these gels gave another unique approach to rapidly analyze cell wall polymer chemistry.

Wheat straw lignin, unlike normal-wood lignins in angiosperm and gymnosperm tree species, derives from all three lignin precursors, p-hydroxycinnamyl alcohol, coniferyl alcohol, and sinapyl alcohol in proportions estimated from thioacidolysis-released monomers to be 5, 49, and 46%, respectively [11, 12]. Enzyme-catalyzed dehydrogenation leads to primarily end-wise polymerization, forming a combinatorial, racemic polymer of phenylpropanoid subunits connected by several types of inter-unit linkages [13]. For example, a sample of milled acetylated wheat straw lignin contained the following familiar linkages: arylglycerol–ß-aryl ethers (ß-O-4), phenylcoumarans (ß–5), resinols (ß–ß), along with cinnamaldehydes, cinnamyl alcohol, and dihydrocinnamyl alcohol end groups [14, 15]. The acidic environment during hydrothermal processes makes it likely that partial hydrolysis of ether linkages will occur. Li et al. [16] described the substantial cleavage of the major lignin ether linkage, in the ß-O-4 units that occurs during the

steam explosion of aspen wood. This same mechanism may occur during the hydrothermal pretreatment of wheat straw [17], but quantification has not been attempted.

The principal hemicelluloses found in wheat straw are the D-xylans, linked β-$(1 \rightarrow 4)$ in xylopyranosyl main chains [18]. In addition, the xylan (ß-D-Xyl$p$) backbone is partially acetylated at the C-2 and C-3 positions. During hydrothermal processes, hydrolysis reactions lead to partial removal of these acetyl groups, thus generating acetic acid which may catalyze the degradation of polysaccharides [19] and, quite possibly, lignin sidechains.

Polysaccharides that intimately associate with lignin in wheat straw have been shown to be the arabinoglucuronoxylans [20], which are comprised of a ß-D-Xyl$p$ unit framework partially substituted at C-2 by 4-O-MeGlcA units, on average two residues per ten ß-D-Xyl$p$ units, and at C-3 by α-L-Ara$f$ units, on average 1.3 residues per ten ß-D-Xyl$p$ units [21]. In *Poaceae, p*-hydroxycinnamates (i.e., p-coumarate, ferulate, and sinapate) are important for the cross-linking of cell wall polymers, providing organization and structural integrity of the wall [22–24]. Ferulate dehydrodimerization [25] and even dehydrotrimerization reactions [26, 27], via radical coupling, produces cross-linking between two polysaccharide chains; the phenolic nature of ferulates or ferulate oligomers makes them amenable to radical coupling into lignin polymers [24, 28]. In grasses, ferulates acylate the C-5 hydroxyl of α-L-arabinofuranosyl units [29, 30]. Ferulate cross-links between arabinoglucuronoxylans and lignin have been found in various cereal grains [31], maize primary walls [32], wheat internodes [33], wheat and oat straw [34], and ryegrass [24], showing the significance of ferulate in lignin–carbohydrate bonding [35]. Dehydrodisinapates and sinapate–ferulate cross-products have been found in various cereal grains and wild rice [36]. A ferulate dehydrotrimer in *Zea mays* L. further solidified the importance of ferulates in cell wall cross-linking [27]. Acylation of lignin sidechains at the primary alcohol (γ–OH) position by p-coumarate has been shown to be about 18% by weight in mature corn lignin [15]. The presence and regiochemistry of p-coumarates on lignins implicates pre-acylation of p-hydroxycinnamyl alcohols during lignification [23, 37, 38].

Here, we describe an enhanced approach to characterize and quantify structural changes in wheat straw from a hydrothermal pretreatment process, before and after enzymatic hydrolysis, using a 2D NMR technique. Analyzing the wheat straw, without derivatization, allows for characterization of cell wall polymers in a fairly native state. Thus, natural acylation of lignin and polysaccharides is fully distinguishable by NMR, permitting identification of specific cell wall polymers and quantification of their changes through hydrothermal and enzymatic treatments.

Materials and Methods

Chemicals

All chemicals used were provided by Aldrich Chemical Company, Milwaukee, WI, USA unless otherwise noted.

Substrates

Wheat straw (*Triticum aestivum* L.) and hydrothermally pretreated wheat straw were supplied by Inbicon A/S, Denmark (www.inbicon.com). Figure 1 shows images of the untreated and hydrothermally pretreated material before and after enzyme hydrolysis, along with SEM images of the material before enzyme hydrolysis. SEM analysis was performed with a FEI Quanta 200 (FEI Company, Eindhoven, The Netherlands) operated at 20 kV, and digital images were recorded. Freeze-dried samples were mounted on aluminum stubs and coated (gold/palladium) with a SC7640 Auto/Manual high-resolution sputter coater (Quorum Technologies, Newhaven, UK).

Chemical Composition Analysis

The composition of solid fractions was analyzed using a two-step strong acid hydrolysis according to an National Renewable Energy Laboratory procedure [39]. Prior to the acid hydrolysis, samples were dried at 40 ℃ for 1–2 days and milled to <1 mm particle size. Dry matter (DM) was determined using a Sartorius MA 30 moisture analyser at 105 ℃. Monosaccharides (D-glucose, D-xylose, and L-arabinose) were quantified on a Dionex Summit high-performance liquid chromatography (HPLC) system equipped with a Shimadzu refractive index detector [40]. Klason lignin content was determined based on the filter cake subtracting the ash content after incinerating the residues from the strong acid hydrolysis at 550 ℃ for 3 h.

Wheat Straw Preparation

Wheat straw was prepared to give samples from four treatment types: untreated control wheat straw (C), hydrothermally pretreated wheat straw (H; solids fraction), hydrolytic enzyme-treated control wheat straw (E; solids fraction), and hydrolytic enzyme-treated hydrothermally pretreated wheat straw (HE; solids fraction). The enzyme hydrolysis was performed to enrich the noncarbohydrate component.

Treatment C was air dried and Wiley milled to 10 mesh and Soxhlet extracted with toluene/ethanol (95%) 1:1.87 (*v/v*) for 12 h to remove waxes and extractives present in cell lumina. All treatments were air dried, then ball-milled using a Retsch (Newtown, PA, USA) PM100 planetary ball mill with ZrO_2 balls and vessel. The ball-milling parameters were: 8 (10 mm) balls+3 (20 mm) balls, 300 rpm, 20 min milling interval followed by 10-min pause, total time of 5 h. Later, the 20-mm balls were replaced with two more 10-mm balls and the speed was increased to 600 rpm. Milling was continued for a total time of 12 h (20 min interval, 10-min pause).

The hydrothermal pretreatment (H) was performed at a feed rate of 75 kgh^{-1} of chopped wheat straw (1–5 cm), which was pre-soaked in water at 80 °C for 6 min [1]. The straw was then held for 6 min in a reactor heated to 195 °C by injection of steam. No chemicals were added. The pretreated biomass was separated by pressing into solid (rich in

Fig. 1 Untreated wheat straw (*top row*); hydrothemally pretreated wheat straw (*bottom row*). Ball-milled wheat straw (*left column*); after ball milling and enzymatic hydrolysis *(middle column);* SEM images after ball milling, but before enzymatic hydrolysis (*right column*) with the white bar indicating 20 μm

Untreated wheat straw

Hydrothermally pretreated wheat straw

C-6 sugars) and liquid fractions (rich in C-5 sugars). The DM content of the solids fraction was 25–32% (*w/w*).

Treatment types E and HE were prepared further by extensive enzymatic hydrolysis to remove polysaccharides; treatment E utilized the extracted material from treatment C. One gram of dried and ball-milled untreated or pretreated wheat straw was incubated separately with Celluclast 1.5 L and Novozyme188 (Novozymes A/S, Bagsværd, Denmark) mixed in a 5:1 (*w/w*) ratio and at 75 filter paper units/g DM at 50 °C (pH4.8). The enzyme preparations contain a range of cellulases and, to a minor extent, hemicellulases. After 3 days of enzymatic hydrolysis, all solids were carefully centrifuged and washed with MilliQ water three times. Hydrolysis was further continued for 3 days with another identical dose of enzyme mixture. For both untreated and pretreated straw, the glucose yields were very close to 100%.

NMR, General

Vacuum-oven dried (40 °C, 3 h) ball-milled wheat straw (all four treatment types, 30 mg each) were added to four individual 5 mm NMR tubes, followed by DMSO-d_6 (500 μl). After sonication, a semiclear solution was formed in approximately 3 h [10]. NMR spectra were acquired at 35 °C on a DMX-500 (^{1}H 500.13 MHz, ^{13}C 125.76 MHz) instrument equipped with a sensitive cryogenically cooled 5 mm TXI ^{1}H/^{13}C/^{15}N gradient probe with inverse geometry. The central DMSO solvent peak was used as an internal reference for all samples δ_C 39.5, δ_H 2.49 ppm). All processing and numerical integration calculations were conducted using Bruker Biospin's TopSpin v. 3.0 (Mac) software. Performing such integrations on NMR data from polymeric materials is sensitive to cross-peak overlap. Thus, all integrations were measured only on intense well-resolved cross-peaks; three separate integration calculations were obtained on each contour within the same sample (at 60, 80, and 120 contour levels) with averages and standard deviations reported.

2D NMR Spectra

A standard adiabatic Bruker pulse sequence implementation (hsqcetgpsisp2.2) was used for acquiring the 2D spectra. The phase-sensitive heteronuclear single quantum coherence (HSQC) spectra were determined with an acquisition time of 170.5 ms using an F2 spectral width of 6,009 Hz (12 ppm) in 2048 data points using 96 transients for each of 500 tl increments of the F1 spectral width of 25,152 Hz (200 ppm) (F1 "acquisition time" of 9.94 ms). Dummy scans (32) were used to establish equilibrium conditions at the start of the experiment. Processing used Gaussian apodization for F2 (LB= −0.18, GB=0.005) and a cosine squared function for F1 prior to 2D Fourier transformation. ^{13}C-Decoupling during acquisition was performed by GARP composite pulses from the high-power output-decoupling channel.

NMR Assignments

All lignin assignments were confirmed with the NMR database of lignin and cell wall model compounds [41] and literature sources [9, 10, 42]. All polysaccharide ^{1}H and ^{13}C chemical shift assignments for the wheat straw species described were assigned using previous literature on wheat straw [43], maize bran (*Z. mays* L.) [10, 27, 42], and aspen wood (*P tremuloides*) [9, 10, 42, 44].

Quantification of Structures by NMR

Quantifying the lignin methoxyl, ß-aryl ether, and polysaccharide *O*-acetyl and uronic acid structures in each sample was performed using the spectral data from 2D NMR. Methoxyl content (millimoles of lignin methoxyls (OMe) per gram of original wheat straw) was calculated based on the chemical composition analysis (Table 1) and a H/G/S ratio of 7:52:41 calculated via NMR integration of the H2/6, G2, and S2/6 contours in the enzyme lignin (E) spectrum (with guaiacyl integrals being logically doubled since they involve only a single correlation rather than the two in the symmetrical H and S units). This ratio closely resembled the ratio determined by Lapierre et al. [12]. Methoxyl content was assumed constant throughout the hydrothermal and enzymatic hydrolysis treatments (see "Results and Discussion" section).

The HSQC NMR spectra of the C, H, E, and HE wheat straw-treated samples were used to determine the ß-aryl ether, 0-acetyl, and uronic acid content. More specifically, the integral for the ^{13}C-^{1}H correlation for the ß-aryl ether α-C/H (Aα), the integral for the ^{13}C-^{1}H correlation for the acetate methyl (−CH$_3$), the two integrals for the ^{13}C-^{1}H correlations for the acetylated xylan structures (2-*O*-Ac-Xyl*p* and 3-*O*-Ac-Xyl*p*), and the integral for the ^{13}C-^{1}H correlation for the anomeric position of 4-*O*-MeGlcA was divided by the integral for the ^{13}C-^{1}H correlation for the OMe, and the resulting ratio was multiplied by the determined molar quantity of OMe per gram of original wheat straw.

Results and Discussion

Chemical Composition

The chemical composition of the wheat straw before and after hydrothermal pretreatment and subsequent enzymatic hydrolysis is presented in Table 1. Hydrothermal pretreatment resulted in a substantial removal of hemicelluloses with a consequent increase in cellulose and Klason lignin content, yielding 740 mg based on 1,000 mg of original

Table 1 Chemical composition of wheat straw before and after hydrothermal pretreatment and enzyme hydrolysis

Substrate[a]	Yield (mg/1,000 mg)	Cellulose (wt%)	Xylan (wt%)	Arabinan (wt%)	Klason lignin (wt%)	Ash (wt%)
Untreated wheat straw (C)	1,000	35.1 (*0.4*)	17.2 (*0.09*)	2.6 (*0.02*)	18.9 (*1.2*)	5.8 (*0.05*)
Hydrothermally pretreated wheat straw (H)	740	49.8 (*0.7*)	8.1 (*0.01*)	ND	29.7 (*1.8*)	3.4 (*0.12*)
Enzyme digested untreated wheat straw (E)[b]	220	–	–	–	–	–
Enzyme digested pretreated wheat straw (HE)	220	ND	ND	ND	79.2 (*1.2*)	17.1 (*0.09*)

Italic numbers are standard deviations

ND none detected

[a] Mannan and galactan were not detectable

[b] Substrate E was not analyzed for composition

wheat straw; the lignin content (Klason lignin in Table 1) showed a 57% increase going from untreated to hydrothermally pretreated wheat straw. Similar results were also observed during hydrothermal, steam explosion, or steam pretreatments of lignocellulosic materials such as corn stover [45], wheat straw [40], and aspen wood [16]. One possible mechanism for the increase in lignin content might be the immediate acid-catalyzed condensation of cleaved lignin moieties in the wheat straw lignin during the hydrothermal process as proposed by Li et al. [16]. The hydrothermal pretreatment removed half the xylan and all the measurable arabinan (Table 1). High-temperature acidic or neutral pretreatments have also been shown to remove hemicelluloses [46] to a large extent and affect the structure and distribution of lignin in the biomass [40, 47, 48]. The organic acids formed during the hydrothermal pretreatment are reported to catalyze the partial hydrolysis of glycosidic bonds in the hemicelluloses producing mono- and oligosaccharides [49]. This removal of hemicelluloses that are physically associated with cellulose may have also resulted in an increase in pore volume [50]. These results demonstrate that high temperature pretreatments (e.g., hydrothermal) can remove hemicelluloses to a large extent and redistribute lignin on the biomass surface. A similar observation was also reported during the alkaline AFEX pretreatment of corn stover [51]. We also showed that the ash content decreased by approximately 40% upon hydrothermal pretreatment as compared to the untreated control (Table 1). However, this is not an uncommon occurrence in hydrothermal processes of wheat straw; similar decreases in ash content were shown by Han et al. during steam explosion of wheat straw [52]. With the increased temperatures and pressures that are employe4 a substantial amount of silica becomes released and mobile. Thus, it is believed that the mobile silica from the wheat straw ends up being washed out in the liquids fraction. After enzymatic hydrolysis of the pretreated sample, the yield decreases to 220 mg based on 1,000 mg of original wheat straw. The enzyme hydrolysis expectedly concentrates the resulting lignin in the hydrothermally pretreated wheat straw, and showed a 167% increase going from the hydrothermally pretreated to the enzyme-digested pretreated wheat straw.

NMR Spectral Regions

Figure 2 displays partial HSQC spectra from all four treatment types (rows) and the spectral regions of interest (columns). Color-coded polymer structures (Fig. 3) correspond to their respective colored spectral contours. The regions displayed include aliphatics from lignin sidechain and non-anomeric polysaccharide correlations (a–d), polysaccharide anomerics (hemicelluloses and cellulose, e–h), and aromatic structures (lignin and hydroxycinnamates, i–l). It is evident from these whole cell wall spectra that major and minor cell wall polymers are represented here for wheat straw with good peak dispersion.

Aliphatic Region

Depicted in Fig. 2a–d are several lignin sidechain correlations found in wheat straw spectra: the major ß-aryl ether units (A, cyan), phenylcoumaran units (B, green), resinol units (C, purple), dibenzodioxocin units (D, red), along with cinnamyl alcohol end-groups (X1, magenta), and lignin methoxyls (−OMe, mocha). The ß-correlations from ß-aryl ether units clearly separate into their respective guaiacyl and syringyl types, shown by Aß$_G$ and Aß$_S$. The ß-aryl ether Aα contour in Fig. 2b is smaller than Aα in Fig. 2a even though the lignin methoxyl contour is scaled to be larger, thus showing qualitative evidence that ß-aryl ether cleavage has occurred. Acylation of the ß-aryl ether γ-hydroxyl with *p*-coumarate (PCA) and acetates, as mentioned in the introduction, is noted here by a (colored) Aγ contour at lower field (higher proton and carbon chemical shifts) than for normal (un-acylated) units [15, 53]. Similarly, phenylcoumaran units are also noted as having been acylated at the γ-hydroxyl with PCA and acetates, by a similarly displaced Bγ contour. Going from Fig. 2a to b
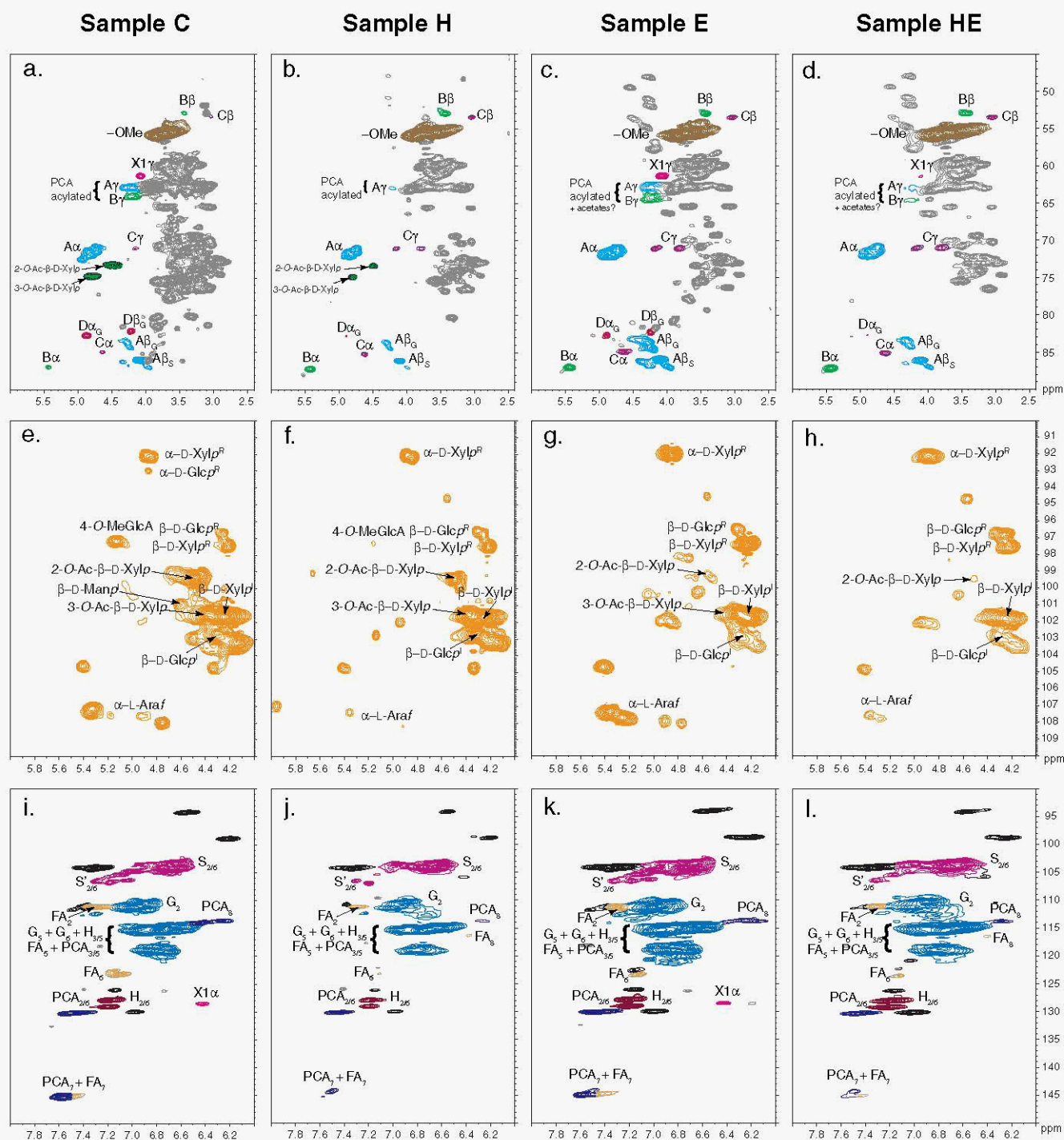
Fig. 2 The aliphatic region (**a–d**), polysaccharide anomeric region (**e–h**), and aromatic region (**i–l**) of ^{13}C–^{1}H correlation (HSQC) spectra of wheat straw. The spectra are aligned vertically to represent each sample treatment as follows: control (sample C), hydrothermally pretreated (sample H), enzyme treated (sample E), and hydrothermally pretreated followed by enzyme treated (sample HE)

and from 2c to d, acylation appears to decrease during the hydrothermal pretreatment process; the higher quality spectra obtainable after cellulase treatment, in Fig. 2c and d, show that some of these linkages do survive the process. Dibenzodioxocin (GG-biphenyl structures) [54–56] units interestingly show some evidence of depletion during the hydrothermal

pretreatment; a structural modification to the dibenzodioxocin units due to the increased acidic conditions during pretreatment may be a potential mechanism [57], but more research is needed to evaluate its fate. Similarly, the cinnamyl alcohol end groups displayed substantial removal. Other lignin groups such as resinols and phenylcoumarans withstand the
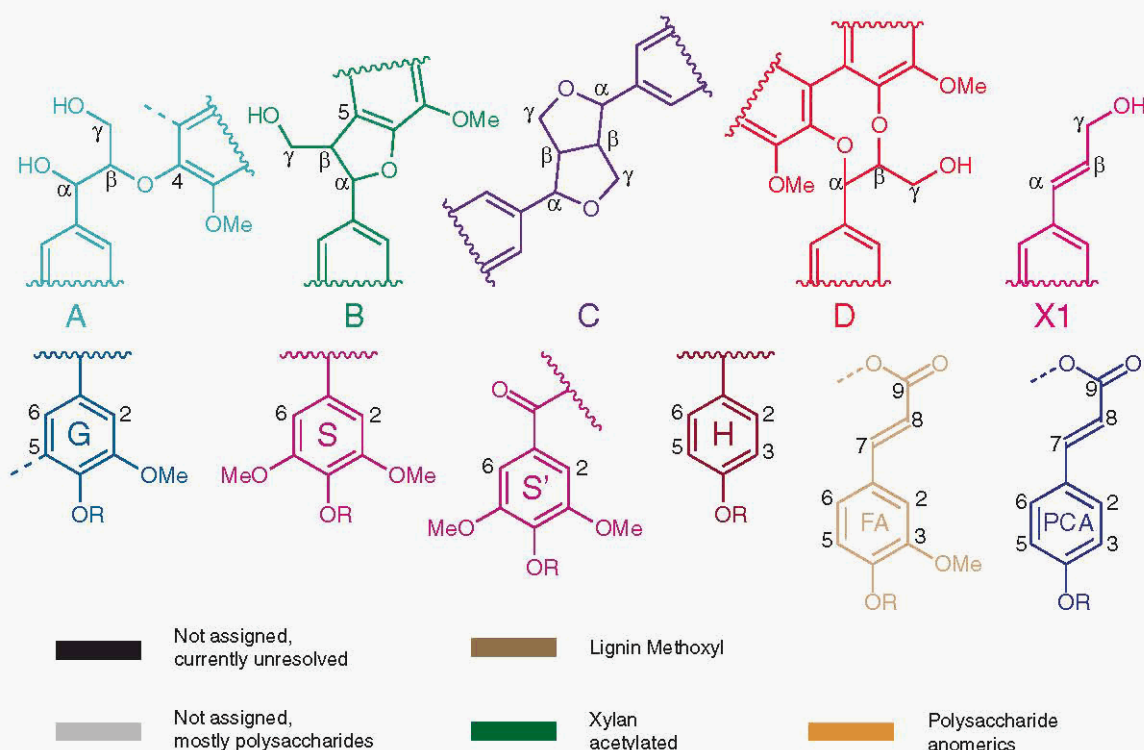
Fig. 3 Key to the chemical structures found in the spectra in Fig. 2. The structures are: **A** β–O–4 (β-aryl ethers) in *cyan*; **B** β–5 (phenylcoumarans) in *green*; **C** β–β (resinols) in *purple*; **D** dibenzodioxocin structures in *red*; **X1** (*E*)-cinnamyl alcohol end groups in *magenta*; **G** guaiacyl units of lignin in *blue*; **S** syringyl units of lignin in *raspberry*; **H** *p*-hydroxyphenyl units in *maroon*; **FA** ferulates in *tan*; and **PCA** *p*-coumarates in *dark blue*. Also shown are *OMe* methoxyls of lignin in *mocha,* polysaccharide anomerics (H1/C1) in *orange, O*-acetylated xylan in *forest green,* unassigned or overlapping contours are in *black,* and other unassigned saccharides etc. are in *gray*

hydrothermal pretreatment process. The 2-*O*-acetylated xylan (2-*O*-Ac-ß-D-Xyl*p*) and the 3-*O*-acetylated xylan (3-*O*-Ac-ß-D-Xylp; forest green) are most abundant in the control whole cell walls of wheat straw, and diminish substantially after hydrothermal pretreatment and even further upon enzymatic hydrolysis (Fig. 2a–d).

Polysaccharide Anomerics

The anomeric region correlations are depicted in Fig. 2e–h in orange, along with tentative assignments of some important polysaccharide anomerics, including (1→4)-linked ß-D-glucopyanosyl units (ß-D-Glc*p*, cellulose), (1→4)-linked ß-D-xylopyranosyl units (ß-D-Xyl*p,* xylan), (1→3)-linked α-L-arabinofuranosyl units (α-L-Ara*p*, arabinan), and negligible amounts of (1→4)-linked ß-D-mannopyanosyl units (ß-D-Man*p*, mannan) in the control. Mannan linkages were detectable in our NMR experiments, but not with HPLC (Table 1); the trace amount of mannan in sample C and the arabinan in sample H and HE may have been hydrolyzed prior to HPLC composition analysis, rendering it undetectable by HPLC. The 2-0-acetylated xylan (2-*O*-Ac-ß-D-Xyl*p*) and the 3-*O*-acetylated xylan (3-*O*-Ac-ß-D-Xyl*p*)

anomerics are also shown here and, as described above, the acetyl groups are removed substantially by the hydrothermal process and even further removal is evidenced after the enzymatic hydrolysis. Glucuronoxylans contain 4-*O*-methyl-α-D-glucuronic acid (4-*O*-MeGlcA) units, which are (1→2)-linked in glucuronoxylans. From Fig. 2e and f, the 4-*O*-MeGlcA seems to be substantially released from the polymer by the hydrothermal pretreatment process. Other polysaccharides show dramatic changes during the hydrothermal pretreatment as well, e.g., the ß-D-Man*p* (Fig. 2e) and the terminal α-L-Ara*p* decrease substantially. Not surprisingly, the ß-D-Glc*p* and the ß-D-Xyl*p* show steadfastness to the hydrothermal pretreatment, displaying their intimate relationship and high resistance to thermal degradation. This is not to say that some glycosidic bond cleavage, and a reduction in the degree of polymerization (DP) of these polymers, is not occurring.

Aromatic Structures

Figures 2i–l depict the lignin aromatic regions, along with the ferulate (FA) and PCA hydroxycinnamates. *Poaceae* species are known to contain not only guaiacyl (G) and syingyl (S) units, but also low levels of *p*-hydroxyphenyl (H) units.

Structure correlations shown include: $S_{2/6}$ and its α-ketone analog $S'_{2/6}$ (raspberry); G_2 (blue); G_5 and G_6 with an overlapping $H_{3/5}$ contour (blue); $H_{2/6}$ (maroon) is shown here well dispersed, PCA_8 and $PCA_{2/6}$ are well dispersed (dark blue), but $PCA_{3/5}$ overlaps with guaiacyl contours and PCA, overlaps with FA,; coloring of PCA, and FA, is meant to indicate rough comparative levels, but not the actual correlation positions. The contour FA_6, and in some cases FA_8, are shown well dispersed (tan), FA, is reasonably well resolved, and FA, overlaps with guaiacyl contours. The disappearance of FA, in the control (Fig. 2i) and untreated enzyme lignin spectra (Fig. 2k) may be due to the lower steric mobility of this C/H bond as compared to the less hindered environment after hydrothermal pretreatment. Cinnamyl alcohol end-groups (X1-α, magenta) appear in the control spectra (Fig. 2i) and, as expected, in the untreated enzyme lignin spectra (Fig. 2k); however, as shown previously for the aliphatic region, X1-α displays complete removal after hydrothermal pretreatment (Fig. 2j and l). Overall, these aromatic spectra suggest that the hydrothermal pretreatment process has not changed lignin aromatics and hydroxycinnamates to any significant degree. whether cinnamate esters (i.e., between arabinoglucuronoxylan C5 primary alcohol and a ferulate carbonyl) may have been cleaved during the hydrothermal process is still to be determined.

NMR Quantification

2D NMR Integration

Two-dimensional HSQC spectra have been used on several occasions to quantify cell wall structures [58-61]. The use of adiabatic pulse sequences, as performed in this study, has the advantage of J independence and offset insensitivity over an essentially unlimited active bandwidth, allowing for quantitative measurements [62,63]. Table 2 summarizes the results of the 2D NMR integration of selected contours. The integration results, as will be discussed in the following sections, allowed for quantifying specific linkages in the HSQC spectra (i.e., for ß-aryl ether units, 2-O-Ac-ß-D-Xyl$p$ and 3-O-Ac-ß-D-Xyl$p$ units, total acetates, and the 4-O-MeGlcA) relative to the lignin methoxyl group. The basis for quantifying structures relative to the lignin methoxyl is due the relatively stable nature of guaiacyl and syringyl methoxyls towards acidolysis, as was reported by Lundquist and Lundgren [64]; only minor amounts of methanol were formed upon acidolysis of lignin. From Table 2, all of the integrals displayed less than 5% error, thus, confirming the precise nature of the technique.

ß-Aryl Ether Linkages

Using the lignin methoxyl content, based on 1,000 mg of the original wheat straw, and the integration data in Table 2 we are able to quantify ß-aryl ether linkages. The quantification results (Table 3) showed that the hydrothermal process depleted ß-aryl ethers from 0.40 to 0.16 mmol; only 40% of their original levels remained. This result for wheat straw is more dramatic compared to a previous study on aspen wood where it was reported that steam explosion at a temperature of 205 °C for 5 min left 63% of its original level of ß-aryl ether linkages intact [16]. Possible reasons for this more severe cleavage with wheat straw are: (1) More latent acid groups (i.e., more acylation by acetate, ferulate, ß-coumarate) are present which help catalyze acidolysis (a typical hydrothermal pretreatment solution has a pH of 4); (2) A lower molecular weight lignin (with lower DP and a higher phenolic content) is more readily "extractable" during pretreatment; (3) Lignin in grasses incorporates more p-hydroxyphenyl (H) units, derived from the incorporation of p-coumaryl alcohol into lignins, than dicots. The increased H units should allow for a higher accessibility of hydrolytic agents as H units are essentially all terminal [12]. The source of these agents, and the possible mechanisms involved, is discussed in the paragraphs to follow. The insignificant decrease in ß-aryl ether linkages after enzymatic hydrolysis (i.e., C to E and H to HE) confirms the highly selective nature of the enzymes toward polysaccharide removal.

O-Acetyl Linkages

Natural acetates found in wheat straw include those on the 2-O-Ac-ß-D-Xyl$p$ and the 3-O-Ac-ß-D-Xyl$p$ units. Using the lignin methoxyl content, based on 1,000 mg of the original wheat straw, and integration data we were able to quantify 0-acetyl linkages. From Table 3, the total acetates after hydrothermal pretreatment showed depletion from 0.62 to 0.12 mmol; i.e., only 19% of the original acetates remained. The total O-Ac-Xyl$p$ acetates depleted from 0.56 to 0.070 mmol. This reveals that most acetates in wheat straw originate from O-Ac-Xyl$p$. However, after hydrothermal pretreatment there are approximately 0.05 mmol of acetates that exist on other structures, suggesting that acetyl group migration onto other cell wall components has likely occurred [65]; such a redistribution was also suggested in a recent ionic liquid system with eucalyptus [66]. Nevertheless, the amount of acetyl cleavage is substantial and would result in ample amounts of acetic acid build-up during the hydrothermal process. After the enzyme hydrolysis of the hydrothermally pretreated wheat straw, the quantity of total acetates decreases even further, going from 0.12 to 0.060 mmol. This result suggests that the enzymatic process cleaves acetates via a different mechanism than the hydrothermal pretreatment process. After both processes, the amount of acetate depletion was 90%.

Table 2 2D NMR contour integration values for ß-aryl ethers, acetates, and uronic acids relative to the lignin methoxyl

Structure	Integration region (^{13}C, ^{1}H ppm)	Control (C)	Hydrothermal (H)	Enzyme (E)	Hydrothermal+enzyme (HE)
Lignin–OCH$_3$	57.9–53.8 4.02–3.37	1	1	1	1
β-aryl ether, Aα	73.3–70.1 5.00–4.65	0.336 (*0.0171*)	0.130 (*0.00497*)	0.325 (*0.00504*)	0.126 (*0.00452*)
Acetate–CH$_3$	22.1–19.3 2.25–1.62	0.519 (*0.00473*)	0.102 (*0.00456*)	0.0831 (*0.00143*)	0.0506 (*0.00121*)
2-O-Ac-Xylp	74.6–72.4 4.62–4.35	0.237 (*0.00900*)	0.0289 (*0.00126*)	a	a
3-O-Ac-Xylp	75.9–73.7 4.92–4.64	0.227 (*0.00580*)	0.0292 (*0.000963*)	a	a
4-O-MeGlcA-1	97.8–96.5 5.25–5.00	0.0367 (*0.00204*)	0.00164 (*0.000110*)	a	a

Italic numbers are standard deviations

[a] Peak too small for accurate determination

Uronic Acids

Uronic acids that are part of 4-*O*-MeGlcA in arabinoglucuronoxylans also displayed substantial losses after the hydrothermal pretreatment as shown in Table 3, going from 0.044 to 0.0020 mmol. This is a 95% depletion after pretreatment. From the anomeric regions of the NMR spectra of the enzymatic hydrolyzates E and HE (Fig. 2g and h), the 4-*O*-MeGlcA contour is no longer present, suggesting that uronic acids are efficiently removed in the enzymatic processes.

Hypothesis of Depletion

Ether cleavage during hydrothermal pretreatment can be hypothesized to occur as follows: (1) Steam temperatures of 195 °C cleave the labile xylan acetyls and 4-*O*-MeGlcA, thus releasing acetic acid and uronic acid; (2) This organic acid build-up leads to acid catalyzed hydrolysis (acidolysis) of ß-aryl ethers and the potential structural modification of dibenzodioxocins and cinnamyl alcohol end groups. Similar mechanisms have been described in the literature where ß-aryl ether cleavage was attributed to organic acid pulping [67–70].

Conclusions

The present study shows that hydrothermal pretreatment increases the cellulose and lignin concentration in the pretreated biomass, mainly due to substantial removal of hemicelluloses, as well as partial removal of extractives and substantial deacylation of lignins and hemicelluloses. Using HSQC ^{13}C–^{1}H correlation NMR spectroscopy, all the major (and some minor) plant cell wall polymers of wheat straw are revealed in a non-derivatized state. From two-dimensional

Table 3 A summary of the 2D NMR analysis results for quantifying ß-aryl ether units, acetates, and uronic acids before and after hydrothermal pretreatment of wheat straw

Substrate	Lignin OMe[a] (wt% of substrate)	Lignin OMe[b] (mmol)	β-aryl ether[b] (mmol)	Acetate–CH$_3$[b] (mmol)	O-Ac-Xylp[b] (mmol)	4-O-MeGlcA[b] (mmol)
Untreated wheat straw (C)	3.70	1.19	0.401 (*0.0205*)	0.621 (*0.00565*)	0.555 (*0.0177*)	0.0439 (*0.00244*)
Hydrothermally pretreated wheat straw (H)	3.70	1.19	0.155 (*0.00594*)	0.122 (*0.00545*)	0.0695 (*0.00266*)	0.00196 (*0.000131*)
Enzyme digested untreated wheat straw (E)	3.70	1.19	0.388 (*0.00602*)	0.0993 (*0.00171*)	–	–
Enzyme digested pretreated wheat straw (HE)	3.70	1.19	0.150 (*0.00540*)	0.060 (*0.00145*)	–	–

Italic numbers are standard deviations

[a] Based on the H, G, and S ratio in the lignin of wheat straw as determined by NMR

[b] Per gram of original wheat straw

integration of specific contours in the NMR spectra, in conjunction with supporting analytical data, the following significant conclusions can be made from the hydrothermal pretreatment based on 1,000 mg of original wheat straw: (1) ß-aryl ether linkages decreased by 60 %; (2) Natural acetyl linkages decreased by 81 %, mostly deriving from Ac-O-Xyl*p*——acetyl migration from Ac-O-Xyl*p* to ß-aryl ethers (Aγ) and phenylcoumarans (Bγ) after enzyme hydrolysis is a logical possibility; (3) Uronic acid from 4-O-MeGlcA decreased by 95%; (4) Some deacylation of *p*-coumarates and ferulates was apparent from the hydrothermal pretreatment as evidenced in the aromatic regions of the HSQC spectra; however, overall, the aromatic region showed very little structural changes in this study. We hypothesize that the high steam temperatures used during the hydrothermal process are sufficient to cleave the labile natural acetates and uronic acids linked along the xylan chain, releasing these organic acids into solution. This acid is then available to catalyze ether hydrolysis, including hydrolysis of ß-aryl ethers, but the syringl/guaiacyl/*p*-hydroxyphenyl distribution remains essentially unaltered.

References

1. Larsen J, Petersen MØ, Thirup L, Li HW, Iversen FK (2008) The IBUS process – lignocellulosic bioethanol close to a commercial reality. Chem Eng Technol 31(5):765–772
2. Aspinall GO (1982) Isolation and fractionation of polysaccharides. In: Aspinall GO (ed) The Polysaccharides, vol 1. Academic, New York, pp 19–35
3. Lai YZ, Sarkanen KV (1971) Isolation and structural studies. In: Sarkanen KV, Ludwig CH (eds) Lignins. Occurrence, formation, structure and reactions. Wiley Interscience, New York, pp 165–240
4. Lu F, Ralph J (2003) Non-degradative dissolution and acetylation of ball-milled plant cell walls: high-resolution solution-state NMR. Plant J 35(4):535–544
5. Forziati FH, Stone WK, Rowen JW, Appel WD (1950) Cotton powder for infrared transmission measurements. J Res Nat Bur Stand 45(2):109–113
6. Schwanninger M, Rodrigues JC, Periera H, Hinterstoisser B (2004) Effects of short-time vibratory ball milling on the shape of FT-IR spectra of wood and cellulose. Vib Spectrosc 36:23–40
7. Fujimoto A, Matsumoto Y, Chang HM, Meshitsuka G (2005) Quantitative evaluation of milling effects on lignin structure during the isolation process of milled wood lignin. J Wood Sci 51:89–91
8. Ikeda T, Holtman K, Kadla JF, Chang HM, Jameel H (2002) Studies on the effect of ball milling on lignin structure using a modified DFRC method. J Agric Food Chem 50(1):129–135
9. Yelle DJ, Ralph J, Frihart CR (2008) Characterization of nonderivatized plant cell walls using high-resolution solution-state NMR spectroscopy. Magn Reson Chem 46:508–517
10. Kim H, Ralph J, Akiyama T (2008) Solution-state 2D NMR of ball-milled plant cell wall gels in DMSO-d_6. Bioenerg Res 1:56–66
11. Lapierre C (2011) Personal Communication
12. Lapierre C, Pollet B, Rolando C (1995) New insights into the molecular architecture of hardwood lignins by chemical degradative methods. Res Chem Intermed 21(3–5):397–412
13. Boerjan W, Ralph J, Baucher M (2003) Lignin biosynthesis. Ann Rev Plant Biol 54:519–546
14. Crestini C, Argyropoulos DS (1997) Structural analysis of wheat straw lignin by quantitative ^{31}P and 2D NMR spectroscopy. The occurrence of ester bonds and α-O-4 substructures. J Agr Food Chem 45:1212–1219
15. Ralph J, Hatfield RD, Quideau S, Helm RF, Grabber JH, Jung HJG (1994) Pathway of *p*-coumaric acid incorporation into maize lignin as revealed by NMR. J Am Chem Soc 116(21):9448–9456
16. Li J, Henriksson G, Gellerstedt G (2007) Lignin depolymerization/repolymerization and its critical role for delignification of aspen wood by steam explosion. Bioresour Technol 98:3061–3068
17. Kaparaju P, Felby C (2010) Characterization of lignin during oxidative and hydrothermal pretreatment processes of wheat straw and corn stover. Bioresour Technol 101:3175–3181
18. Buchala AJ, Wilkie KCB (1973) Total hemicelluloses from wheat at different stages of growth. Phytochemistry 12:499–505
19. Garrote G, Domínguez H, Parajó JC (1999) Hydrothermal processing of lignocellulosic materials. Holz als Roh- und Werkst 57:191–202
20. Scalbert A, Monties B, Lallemand J-Y, Guittet E, Rolando C (1985) Ether linkage between phenolic acids and lignin fractions from wheat straw. Phytochemistry 24(6):1359–1362
21. Sjöström E (1993) Wood Chemistry: fundamentals and applications, 2nd edn. Academic Press, Inc., San Diego
22. Fry SC, Miller JG (1989) Toward a working model of the growing plant cell wall: phenolic cross-linking reaction in the primary cell walls of dicotyledons. In: Lewis NG, Paice MG (eds) Plant cell wall polymers: biogenesis and biodegradation, vol ACS, Symposium Series 399. American Chemical Society, Washington, D.C., pp 33–46
23. Ralph J (2010) Hydroxycinnamates in lignification. Phytochem Rev 9:65–83
24. Ralph J, Grabber JH, Hatfield RD (1995) Lignin-ferulate cross-links in grasses – active incorporation of ferulate polysaccharide esters into ryegrass lignins. Carbohydr Res 275(1):167–178
25. Ralph J, Quideau S, Grabber JH, Hatfield RD (1994) Identification and synthesis of new ferulic acid dehydrodimers present in grass cell-walls. J Chem Soc Perk T 1(23):3485–3498
26. Bunzel M, Heuermann B, Kim H, Ralph J (2008) Peroxidase-catalyzed oligomerization of ferulic acid esters. J Agr Food Chem 56:10368–10375
27. Bunzel M, Ralph J, Funk C, Steinhart H (2003) Isolation and identification of a ferulic acid dehydrotrimer from saponified maize bran insoluble fiber. Eur Food Res Technol 217(2):128–133
28. Quideau S, Ralph J (1997) Lignin-ferulate cross-links in grasses 4. Incorporation of 5-5-coupled dehydrodiferulate into synthetic lignin. J Chem Soc Perk T 1 1(16):2351–2358
29. Hatfield RD, Ralph J, Grabber JH (1999) Cell wall cross-linking by ferulates and diferulates in grasses. J Sci Food Agr 79(3):403–407
30. Mueller-Harvey I, Hartley RD, Harris PJ, Curzon EH (1986) Linkage of *p*-coumaryl and feruloyl groups to cell wall polysaccharides of barley straw. Carbohydr Res 148:71–85
31. Bunzel M, Ralph J, Lu F, Hatfield RD, Steinhart H (2004) Lignins and ferulate-coniferyl alcohol cross-coupling products in cereal grains. J Agr Food Chem 52(21):6496–6502
32. Grabber JH, Ralph J, Hatfield RD (2002) Model studies of ferulate-coniferyl alcohol cross-product formation in primary

maize walls: implications for lignification in grasses. J Agr Food Chem 50(21):6008–6016

33. Iiyama K, Lam TBT, Stone BA (1990) Phenolic acid bridges between polysaccharides and lignin in wheat internodes. Phytochemistry 29:733–737

34. Jacquet B, Pollet B, Lapierre C, Mhamdi F, Rolando C (1995) New ether-linked ferulic acid-coniferyl alcohol dimers identified in grass straws. J Agr Food Chem 43:2746–2751

35. Ralph J, Bunzel M, Marita JM, Hatfield R, Lu F, Kim H et al (2004) Peroxidase-dependent cross-linking reactions of p-hydroxycinnamates in plant cell walls. Phytochem Rev 3:79–96

36. Bunzel M, Ralph J, Kim H, Lu FC, Ralph SA, Marita JM et al (2003) Sinapate dehydrodimers and sinapate-ferulate heterodimers in cereal dietary fiber. J Agr Food Chem 51(5):1427–1434

37. Lu F, Ralph J (1999) Detection and determination of p-coumaroylated units in lignins. J Agr Food Chem 47(5):1988–1992

38. Ralph J, Landucci L (2010) NMR of lignins. In: Heitner C, Dimmel DR, Schmidt JA (eds) Lignin and Lignans: advances in chemistry. CRC Press (Taylor & Francis Group), Boca Raton, pp 137–234

39. Sluiter A (2004) Determination of structural carbohydrates and lignin in biomass. http://www.nrel.gov/biomass/analytical_procedures.html. National Renewable Energy Laboratory (NREL) Analytical Procedures

40. Kristensen JB, Thygesen LG, Felby C, Jørgensen H, Elder T (2008) Cell-wall structural changes in wheat straw pretreated for bioethanol production. Biotechnol Biofuels 1(5):1–9

41. Ralph SA, Ralph J, Landucci LL (2004) NMR database of lignin and cell wall model compounds, http://ars.usda.gov/Services/docs.htm?docid=10491

42. Kim H, Ralph J (2010) Solution-state 2D NMR of ball-milled plant cell wall gels in DMSO-d₆/pyridine-d₅. Org Biomol Chem 8 (3):576–591

43. Sun XF, Sun R, Fowler P, Baird MS (2005) Extraction and characterization of original lignin and hemicelluloses from wheat straw. J Agr Food Chem 53:860–870

44. Teleman A, Lundqvist J, Tjerneld F, Stalbrand H, Dahlman O (2000) Characterization of acetylated 4-O-methylglucuronoxylan isolated from aspen employing ¹H and ¹³C NMR spectroscopy. Carbohydr Res 329(4):807–815

45. Selig MJ, Viamajala S, Decker SR, Tucker MP, Himmel ME, Vinzant TB (2007) Deposition of lignin droplets produced during dilute acid pretreatment of maize stems retards enzymatic hydrolysis of cellulose. Biotechnol Prog 23:1333–1339

46. Mosier NS, Hendrickson R, Brewer M, Ho N, Sedlak M, Dreshel R et al (2005) Industrial scale-up of pH-controlled liquid hot water pretreatment of corn fiber for fuel ethanol production. Appl Biochem Biotechnol 125:77–97

47. Donohoe BS, Tucker MP, Davis M, Decker SR, Himmel ME, Vinzant TB (2007) Tracking lignin coalescence and migration through plant cell walls during pretreatment, vol 5B-01. 29th Symposium on Biotechnology for Fuels and Chemicals. Denver, CO

48. Hansen MA, Kristensen JB, Felby C, Jørgensen H (2011) Pretreatment and enzymatic hydrolysis of wheat straw (Triticum aestivum L.) – the impact of lignin relocation and plant tissues on enzymatic accessibility. Bioresour Technol 102:2804–2811

49. Kabel MA, Bos G, Zeevalking J, Voragen AGJ, Schols HA (2007) Effect of pretreatment severity on xylan solubility and enzymatic breakdown of the remaining cellulose from wheat straw. Bioresour Technol 98:2034–2042

50. Grethlein HE (1985) The effect of pore size distribution on the rate of enzymatic hydrolysis of cellulosic substrates. Nat Biotechnol 3 (2):155–160

51. Chundawat SPS, Donohoe BS, da Costa SL, Elder T, Agarwal UP, Lu F et al (2011) Multi-scale visualization and characterization of lignocellulosic plant cell wall deconstruction during thermochemical pretreatment. Energy Environ Sci. doi:10.1039/c1030ee00574f

52. Han G, Deng J, Zhang S, Bicho P, Wu Q (2010) Effect of steam explosion treatment on characteristics of wheat straw. Ind Crop Prod 31(1):28–33

53. Ralph J, Marita JM, Ralph SA, Hatfield R, Lu F, Ede RM et al (1999) Solution-state NMR of lignins. In: Argyropoulos DS, Rials T (eds) Advances in lignocellulosics characterization. TAPPI Press, Atlanta, pp 55–108

54. Akiyama T, Kim H, Dixon RA, Ralph J (2007) Dibenzodioxocin structures involving p-hydroxyphenyl units in C3H down-regulated lignin. In: 10th International Congress on Biotechnology in the Pulp and Paper Industry. Madison, WI, p 71

55. Ämmälahti E, Brunow G, Bardet M, Robert D, Kilpeläinen I (1998) Identification of side-chain structures in a poplar lignin using three-dimensional HMQC-HOHAHA NMR spectroscopy. J Agr Food Chem 46(12):5113–5117

56. Karhunen P, Rummakko P, Sipilä J, Brunow G, Kilpeläinen I (1995) Dibenzodioxocins; a novel type of linkage in softwood lignins. Tetrahedron Lett 36:169–170

57. Karhunen P, Rummakko P, Pujunen A, Brunow G (1996) Synthesis and crystal structure determination of model compounds for the dibenzodioxocine structure occurring in wood lignins. J Chem Soc Perk T 1(18):2303–2308

58. Stewart JJ, Akiyama T, Chapple C, Ralph J, Mansfield SD (2009) The effects on lignin structure of overexpression of ferulate 5-hydroxylase in hybrid poplar. Plant Physiol 150:621–635

59. Wagner A, Donaldson L, Kim H, Phillips L, Flint H, Steward D et al (2009) Suppression of 4-coumarate-CoA ligase in the coniferous gymnosperm Pinus radiata. Plant Physiol 149(1):370–383

60. Yelle DJ, Ralph J, Frihart CR (2011) Delineating pMDI model reactions with loblolly pine via solution-state NMR spectroscopy. Part 2. Non-catalyzed reactions with the wood cell wall. Holzforschung 65:145–154

61. Zhang LM, Gellerstedt G (2007) Quantitative 2D HSQC NMR determination of polymer structures by selecting suitable internal standard references. Magn Reson Chem 45:37–45

62. Koskela H, Heikkilä O, Kilpeläinen I, Heikkinen S (2010) Quantitative two-dimensional HSQC experiment for high magnetic field NMR spectrometers. J Magn Reson 202:24–33

63. Kupče E, Freeman R (2007) Compensated adiabatic inversion pulses: broadband INEPT and HSQC. J Magn Reson 187:258–265

64. Lundquist K, Lundgren R (1972) Acid degradation of lignin. Part VII. The cleavage of ether bonds. Acta Chem Scand 26(5):2005–2023

65. Reicher F, Corrêa JBC, Gorin PAJ (1984) Location of O-acetyl groups in the acidic D-xylan of Mimosa scabrella (bracatinga). A study of O-acetyl group migration. Carbohydr Res 135:129–140

66. Çetinkol ÖP, Dibble DC, Cheng G, Kent MS, Knierim B, Auer M et al (2010) Understanding the impact of ionic liquid pretreatment on eucalyptus. Biofuels 1:33–46

67. Ede RM, Brunow G, Poppius K, Sundquist J, Hortling B (1988) Formic acid/peroxyformic acid pulping. 1. Reactions of β-aryl ether model compounds with formic acid. Nord Pulp Pap Res J 3 (3):119–123

68. Nimz HH, Robert D (1985) 13C NMR spectra of acetic acid lignins. In: International Symposium on Wood and Pulping Chemistry. Vancouver, B.C., p 267

69. Sarkanen KV (1980) Acid catalyzed delignification of lignocellulosics in organic solvents. In: Sarkanen KV, Tillman DA (eds) Progress in biomass conversion, vol 2. Academic, New York, pp 127–144

70. Shimada K, Hosoya S, Tomimura Y (1991) Delignification with organic acids. In: International Symposium on Wood and Pulping Chemistry. TAPPI Press, Melbourne, pp 183–188